Multi-timescale exploration of teleconnection/tornado activity relationships in the Southeastern United States

Todd W. Moore

twmoore@fhsu.edu

Fort Hays State University

Tiffany A. DeBoer

Tyler Fricker

University of Louisiana Monroe

Research Article

Keywords: Tornadoes, Teleconnections, Interactions, Seasonality, Southeastern United States

Posted Date: February 8th, 2024

DOI: https://doi.org/10.21203/rs.3.rs-3935656/v1

Additional Declarations: No competing interests reported.

Version of Record: A version of this preprint was published at Theoretical and Applied Climatology on April 13th, 2024. See the published version at https://doi.org/10.1007/s00704-024-04960-4.

Abstract

Teleconnections like the El Niño/Southern Oscillation affect climate and weather conditions across the globe, including conditions that modulate tornado activity. Early studies of teleconnection/tornado activity relationships provided evidence of links between one teleconnection and tornado activity. Later attempts introduced multivariate approaches by analyzing bivariate distributions and integrating multiple teleconnections in statistical models to predict variability in tornado activity. However, little attention has been given to teleconnection interactions and the role of these interactions in modulating tornado activity. Here, we employ a data-driven, multiple logistic regression modelling approach to explore the interactions between the El Niño/Southern Oscillation, North Atlantic Oscillation, Artic Oscillation, and Pacific North American pattern and their ability to predict the odds of an active tornado period in the southeastern United States. We develop models at the annual, seasonal, and monthly scales and, in doing so, illustrate that the teleconnections and teleconnection interactions that best predict the odds of an active tornado period differ across timescales and that the relationships exhibit clear seasonality. We also show climate conditions associated with select interactions that help explain the elevated tornado activity, namely anomalously high near-surface air temperature and humidity steered by an anomalously strong subtropical high.

1 Introduction

Tornadoes are narrow, violently rotating columns of air that extend from a thunderstorm to the ground (Glickman 2000). They occur throughout the world, but are most common in the United States (US), which experiences more than 1,200 a year, on average, especially east of the Rocky Mountains (SPC 2018). Tornadoes are destructive to human development as well as fatal for human life. For example, the average annual economic loss from tornadoes was $982 million between 1949 and 2006 (Changon 2009) and while there has been a decline in fatalities over time (Brooks and Doswell 2002; Ashley 2007; Fricker and Friesenhahn 2022), the average annual fatality rate between 1995 and 2018 is 74 (Fricker and Friesenhahn 2022).

Studies that document the spatiotemporal distributions and shifts in tornado activity in the US show that the Southeast (SE) region is particularly tornado prone (Dixon et al. 2011; Coleman and Dixon 2014; Agee et al. 2016; Ashley and Strader 2016; Gensini and Brooks 2018; Moore 2018; Moore and DeBoer 2019). Societal exposure is also high in the SE due to denser population, urban land use, and non-permanent and non-attached housing units (Cutter et al. 2003; Ashley and Strader 2016; Strader et al. 2017). The coupling of relatively high risk and exposure sets the stage for high tornado vulnerability in the SE US under the framework of place-based vulnerability (Cutter et al. 2003; Fricker and Elsner 2019). Due to the high vulnerability, it is important to understand the variability of tornado activity, and the drivers of variability, to improve monthly and seasonal outlooks and to mitigate losses.

Some studies have sought links between large-scale climate patterns and tornadoes to predict whether an extended period (e.g., month or season) will be active or inactive. Such monthly or seasonal outlooks

(e.g., Allen et al. 2015; Lepore et al. 2017) could allow state and local agencies to communicate with the public to raise awareness and preparedness. The El Niño/Southern Oscillation (ENSO), which is linked to tornado activity via modulations in the jet stream (Allen et al. 2015; Cook et al. 2017; Lepore et al. 2017) and environmental ingredients that favor tornadoes (i.e., moisture, instability, shear, and lift), has been a focus of these efforts. Different metrics of ENSO have shown skill in predicting tornado activity (Allen et al. 2015; Lepore et al. 2017; Moore 2019), but, although skillful, ENSO does not account for much of the variability observed in tornado activity (Marzban and Schaefer 2001) and active (inactive) periods do occur when the ENSO state is unfavorable (favorable) for tornadoes (Moore et al. 2018). Furthermore, in the continuum of the atmosphere, ENSO interacts with other atmospheric teleconnections that also alter the jet stream and tornado ingredients (Deser 2000; Alexander et al. 2002): the Pacific-North American Oscillation (PNA) (Muñoz and Enfield 2011), the North Atlantic Oscillation (NAO) (Muñoz and Enfield 2011; Elsner et al. 2016), and the Artic Oscillation (AO) (Childs et al. 2018). These teleconnections, therefore, should be considered with ENSO to determine if they improve the predictability of tornado activity. This is important in all regions impacted by tornadoes, but especially in the SE US where tornado risk and vulnerability are high and perhaps increasing (Cutter et al. 2003; Agee et al. 2016; Ashley and Strader 2016; Strader et al. 2017; Gensini and Brooks 2018; Moore 2018; Moore and DeBoer 2019; Fricker and Elsner 2019) and where the connection between tornadoes and some teleconnections has been shown to be relatively strong (Allen et al. 2015; Elsner et al. 2016; Lepore et al. 2017; Childs et al. 2018; Moore 2019; Nouri et al. 2021).

Other studies have explored the relationship between multiple teleconnections and US tornadoes. For example, Elsner et al. (2016) analyzed springtime ENSO, NAO, and sea surface temperature in the Gulf of Alaska and western Caribbean to assess seasonal tornado risk. Childs et al. (2018) analyzed cold season tornado activity in relation to ENSO and AO, while DeBoer (2019) generated multivariate statistical models using ENSO, NAO, AO, and PNA to predict the odds of an active tornado month. Nouri et al. (2021) also analyzed a suite of teleconnections in relation to annual tornado activity across different US states and regions, but their approach built on previous efforts by including teleconnection interactions. Tippett et al. (2022) also recently examined the interaction between ENSO and AO on a tornado environment index, but for only February, March, and April.

While this body of literature illustrates the potential of teleconnections to help predict tornado activity, it is spread over different timescales and periods and yields variable results. Missing from this body is a comprehensive analysis of the relationship between tornado activity and multiple teleconnections and their interactions, at multiple timescales. In response, here we propose a regional data-driven modeling framework that exists annually, seasonally, and monthly. Our study aligns with this growing body of literature but takes a more exploratory approach by using stepwise multiple logistic regression to identify the most parsimonious model composed of a teleconnection, suite of teleconnections, or teleconnection interactions that best predicts the odds of an active tornado period across different timescales. In doing so, we suggest that the tornado/teleconnection relationship is statistically scale dependent and seasonal. We also illustrate a way to explore teleconnection interactions to guide future

climatological/meteorological research into the physical mechanisms that may be driving such statistical interactions.

2 Data and Methods

We use tornado data from the Storm Prediction Center's (SPC) Severe Weather Database (SPC 2018). Only tornadoes that occurred within the SE US during the period 1954–2022 were considered. We define the SE as the state boundaries of Arkansas, Alabama, Georgia, Florida, Kentucky, Louisiana, Mississippi, North Carolina, South Carolina, Tennessee, and Virginia, consistent with prior work (Fig. 1) (Guo et al. 2016; Moore 2018). Furthermore, only those tornadoes rated 1 or higher by the Fujita damage scale prior to 1 February 2007 or the Enhanced Fujita damage scale thereafter (E(F) scales hereafter) were considered to reduce the influence of non-meteorological factors on the time series (Verbout et al. 2006). And though the record of E(F)1 + tornadoes includes low-frequency variability, no long-term trend exists (Moore and DeBoer 2019) as compared to the record of E(F)0 + tornadoes.

Several teleconnection indices are used as a means of linking weather patterns across space (Table 1). Sea surface temperature (SST) anomalies averaged over the Niño 3.4 region (5°S–5°N, 170°–120°W) were taken from NOAA Earth System Research Laboratory to represent ENSO (NOAA 2018b). Niño 3.4 SST anomalies serve as the basis of the Oceanic Niño Index (ONI), the 3-month running mean of SST anomalies in the Niño 3.4 region and has been used in tornado studies (Allen et al. 2015; Lepore et al. 2017). The Niño 3.4 index is documented at the monthly scale and was preferred in this study over ONI because the relationships between tornado counts and ENSO were examined at the monthly rather than seasonal scale. PNA, NAO, and AO indices were taken from Climate Prediction Center (NOAA 2018b). PNA and NAO are represented by monthly standardized 500-mb geopotential height anomalies. AO is represented by monthly standardized 1000-mb geopotential height anomalies.

Table 1
Description of teleconnections phases and their influence in the SE.

Teleconnection	Definition	Impacts in the Southeast
ENSO	Coupled oceanic-atmosphere circulation between the eastern and western equatorial Pacific Ocean (NOAA 2018a).	EN phase: Southwesterly jet stream leading to more frequent midlatitude cyclones (Smith et al. 1996). LN phase: Temperatures increase and low-level jets advect moisture from the Gulf of Mexico into the coastal states (Gilford et al. 2013).
NAO	Circulation pattern mainly confined to the extratropics involving the pressures between the Bermuda-Azores High and Icelandic Low (Barry 2001).	Positive phase: Bermuda High and Icelandic Low are enhanced strengthening the westerlies aloft raising surface temperatures (Ting et al. 1996). Negative phase: Weakening of jet stream leading to more frequent midlatitude cyclones over the SE (Ting et al. 1996).
AO	Modulation in the strength of the circumpolar vortex aloft (Thompson and Wallace 1998).	Positive phase: Strengthened polar jet correlates with increases in severe weather due to moisture influxes and increased wind shear in the SE (Childs et al. 2018). Negative phase: Polar westerlies aloft weaken and advect cold air from the Arctic into the SE creating large horizontal temperature gradients (Childs et al. 2018).
PNA	Relative amplitudes of the ridge and trough over North America involving pressures over central Pacific Ocean, western Canada, and the southeastern US (NOAA 2018b).	Positive phase: Increased meridional flow of the jet stream resulting cool outbreaks and increases in midlatitude cyclone frequency (Leathers et al. 1991). Negative phase: Increased zonal flow of the jet stream and is shifted northward increasing temperature and moisture influxes from the Gulf of Mexico (Leathers et al. 1991).

Statistical models are fit to probabilities of tornado activity. In particular, we apply multiple logistic regression to explore whether combinations of teleconnections or their interactions can predict the odds of an active tornado period. Rather than predicting tornado counts, logistic regression allows us to determine if some combination of teleconnections or their interactions can predict the odds of tornado activity being above or below *normal* for the period under consideration. Normal, in this study, is represented by the median tornado counts of three 23-year periods (Period 1 = 1954–1976; Period 2 = 1977–1999; Period 3 = 2000–2022) to account for non-stationarity, with an *active* period defined as one

in which the number of tornadoes is greater than the median and an *inactive* period as one in which the number of tornadoes is less than or equal to the median.

Here, three sets of models are evaluated: (1) annual model, (2) seasonal models, and (3) monthly models. To account for the potential joint effects of teleconnections on tornado activity, we expand a traditional fixed modeling framework to include interaction terms between the individual teleconnections. Doing this allows for a modeling framework that is more flexible than a series of fixed terms and provides the ability to interpret the relationship between one teleconnection and tornado activity through different values of another teleconnection. The addition of interaction terms in regression analysis has been shown to improve model results in tornado casualties (Elsner et al. 2018) and makes physical sense, here, when considering the influence multiple teleconnections might have on underlying weather patterns across space and time. The models are all given as:

$$\log\left(\frac{p\left(A\right)}{1-p\left(A\right)}\right)=\beta_1 Month+\beta_2 ENSO+\beta_3 AO+\beta_4 NAO+\beta_5 PNA$$

,

where *p(A)* is the probability of tornado activity (*A*) at an annual, seasonal, or monthly scale, *ENSO* is the Niño 3.4 SST, *AO* is Arctic Oscillation, *NAO* is the North Atlantic Oscillation, and *PNA* is the Pacific-North American pattern. The interaction terms are formally expressed by a colon and indicate which two teleconnections are evaluated across the entirety of their range of values. Important for this work, the seasonal and monthly models are found through a subset of tornadoes occurring during each season or month across the three 23-year periods. This means inference on the model coefficients *might* be best served to employ a Bonferroni correction, which accounts for multiple comparisons—albeit still in a conservative fashion.

Given our exploratory approach with the goal of identifying the most parsimonious model for the prediction of tornado activity, we use a stepwise selection process, in both the forward and backward directions, to identify the model with the lowest Akaike Information Criteria (AIC) (Gorsevski et al. 2006; Chaurasia and Harel 2012; Gijben et al. 2017). In short, we look to select the model that best fits the data with the least number of predictors. Given the range of teleconnections that have been reported to influence tornado activity, we begin with models that include all teleconnections along with all possible interaction terms. The models yield predicted probabilities of an active period based on teleconnection index values. Assessing these predicted probabilities, specifically identifying teleconnections or teleconnection interactions that are associated with a probability of an active month that is > 50% allows us to determine whether these teleconnections improve upon pure chance. If a stepwise selection process results in the return of only an intercept, we infer that no teleconnection aids in the prediction of tornado activity.

Data-driven exploratory approaches like this one provide insight into statistical relationships that can guide research into physical mechanisms. While a comprehensive analysis of physical mechanisms is

beyond the scope of this study, we use monthly anomaly composites from the 20th Century Reanalysis version 3 dataset (https://psl.noaa.gov/cgi-bin/data/composites/plot20thc.v2.pl) to illustrate how our approach can guide focused analyses of climate conditions associated with teleconnection interactions that are statistically linked to active tornado periods. We focus on 850-mb geopotential height, 2-m air temperature, and 2-m specific humidity to characterize the large-scale pattern and low-level thermodynamic background conditions that are associated with select teleconnection interactions.

3 Results

Results for the most parsimonious annual, seasonal, and monthly models are summarized in Table 2. *Beta* coefficients for independent predictors describe the log-odds of a year being active relative to a one-unit change in the predictor while holding other predictors constant. Positive coefficients suggest that the log-odds of an active timescale increase as the teleconnection index increases, whereas negative coefficients suggest that the log-odds of an active timescale decrease as the teleconnection index increases. Odds ratios are found using the exponential of the *beta* coefficients for the independent predictors. Odds ratios that are greater than 1 suggest that the odds of an active timescale increase along with the teleconnection index whereas those that are less than 1 suggest that the odds of an active timescale increase when the teleconnection index decreases.

Beta coefficients for interactive terms describe the log-odds of a timescale being active depending on the values of *both* predictors in the interaction. For example, a positive *beta* coefficient suggests that the probability of an active timescale increases with increasing values of both predictors, while a negative *beta* coefficient suggests that the probability of an active timescale decreases as a function of one predictor with increasing values of the other predictor. The odds ratios of interactive terms are more difficult to infer than independent predictors, as no single value can describe the entirety of an interaction, but should be thought of as an average odds ratio, given all possible values of the included predictors.

With the goal of producing the most parsimonious models, as identified by AIC, we do not perform any adjustments to alpha to control the family-wise error. In addition, we do not focus on probability values (*p*-values), so as to select models that are the most data-driven without incurring issues of overfitting.

Table 2
Summary of logistic regression models.

Period	Selected predictors	*Beta* Coefficients	Standard error	Odds ratio	*p*-value	AIC
Annual						
	AO	3.60	1.24	36.82	0.003	90.89
	NAO	-2.09	1.18	0.1315	0.09	
	PNA	-1.21	0.90	0.30	0.18	
	AO:NAO	-2.91	2.21	0.05	0.19	
	AO:PNA	-4.51	2.55	0.01	0.08	
Seasonal						
DJF	AO	1.41	0.48	4.11	0.003	87.35
	NAO	-1.53	0.64	0.32	0.07	
	AO:NAO	-0.82	0.52	0.44	0.12	
MAM	ENSO	-0.53	0.50	0.59	0.29	92.14
	NAO	-1.45	0.67	.24	0.03	
	ENSO:NAO	-2.41	1.10	0.9	0.03	
JJA	PNA	-0.76	0.39	0.47	0.05	95.45
SON	ENSO	0.01	0.31	1.01	0.98	100.51
	AO	0.33	0.78	1.39	0.67	
	NAO	-0.78	0.56	0.46	0.16	
	PNA	0.01	0.49	1.01	0.98	
	ENSO:AO	-1.28	0.70	0.28	0.07	
	AO:PNA	-1.62	1.16	0.20	0.16	
Monthly						
January	ENSO	0.39	0.27	1.47	0.15	96.14
	AO	0.14	0.26	1.16	0.57	
	NAO	0.20	0.40	1.23	0.61	
	PNA	-0.77	0.36	0.46	0.03	
	AO:NAO	-0.32	0.20	0.73	0.11	

Period	Selected predictors	*Beta* Coefficients	Standard error	Odds ratio	*p*-value	AIC
February	ENSO	-0.53	0.37	0.59	0.15	98.68
	AO	0.47	0.31	1.60	0.13	
	NAO	-0.42	0.45	0.66	0.35	
	PNA	-0.04	0.32	0.96	0.90	
	ENSO:NAO	-0.53	0.34	0.59	0.11	
	ENSO:PNA	0.89	0.43	2.44	0.04	
March	ENSO	-0.66	0.37	0.51	0.07	91.57
	NAO	0.60	0.28	1.82	0.03	
April	ENSO	-0.35	0.54	0.71	0.52	101.76
	AO	0.01	0.44	1.01	0.99	
	NAO	-0.44	0.33	0.65	0.18	
	PNA	0.29	0.34	1.34	0.39	
	ENSO:AO	1.10	0.8	3.01	0.17	
	ENSO:NAO	-1.79	0.8	0.17	0.03	
	AO:PNA	-0.67	0.47	0.51	0.15	
	NAO:PNA	0.54	0.37	1.72	0.15	
May	ENSO	-1.14	0.59	0.32	0.05	94.59
	AO	-1.05	0.64	0.35	0.1	
	NAO	-0.51	0.36	0.60	0.16	
	PNA	-0.27	0.35	0.76	0.43	
	ENSO:AO	-2.27	1.05	0.10	0.03	
	ENSO:PNA	-1.55	0.69	0.21	0.02	
June	ENSO	1.36	0.67	3.89	0.04	93.09
	AO	-0.04	1.01	0.96	0.96	
	NAO	0.04	0.52	1.04	0.93	
	PNA	-0.93	0.38	0.39	0.01	
	ENSO:AO	-4.45	2.09	0.01	0.03	

Period	Selected predictors	*Beta* Coefficients	Standard error	Odds ratio	*p*-value	AIC
	ENSO:NAO	1.88	1.15	6.54	0.10	
July	PNA	-0.41	0.25	0.67	0.09	96.41
August	Intercept only					
September	ENSO	-0.18	0.33	0.83	0.58	100.24
	PNA	-0.12	0.27	0.89	0.66	
	ENSO:PNA	0.55	0.38	1.74	0.14	
October	Intercept only					
November	ENSO	-0.08	0.27	0.93	0.77	101.34
	AO	0.29	0.41	1.34	0.47	
	NAO	-0.50	0.39	0.61	0.20	
	PNA	0.22	0.31	1.25	0.47	
	ENSO:NAO	0.46	0.28	1.59	0.09	
	ENSO:PNA	0.61	0.33	1.84	0.06	
	AO:PNA	-0.51	0.36	0.60	0.15	
December	NAO	-0.36	0.24	0.70	0.14	97.21

3.1 Annual model

We estimate the annual model using our data set of 828 unique combinations of year, month, and period. In the annual model stepwise selection process, AO, NAO, PNA, and the AO:NAO and AO:NA interactions are selected as predictors (Table 2). This suggests that over the study period, AO, NAO, and PNA best predict the level of tornado activity at the annual scale across the SE US.

The odds ratios of the annual model indicate that the probability of an active tornado year decreases with AO as values of the NAO index increase. Similarly, the probability of an active tornado year decreases with AO as values of the PNA index increase. That said, as values of AO increase, so does the probability of an active year, regardless of the value of an interacting NAO or PNA index. In fact, when predicting annual tornado activity as a function of AO, the probability of an active year moves from near 0% for an AO value of − 1 to near 100% with an AO value of 1 across the entire interquartile range of NAO and PNA values (Fig. 2). This suggests that years dominated by positive AO are more likely to have more active periods—when accounting for all teleconnections and interactions.

3.2 Seasonal models

We estimate the seasonal model using a data set of 276 unique combinations of year, season, and period. Seasons are defined by three-month groups commonly found in the literature: (1) December, January, and February (DJF), (2) March, April, and May (MAM), (3) June, July, and August (JJA), and (4) September, October, and November (SON).

AO:NAO and AO:PNA interactions are suggested to be most associated with tornado activity in the annual model. The MAM and SON seasonal models include ENSO, which was not included in the annual model. Furthermore, the seasonal modelling approach captures teleconnection interactions that are not selected in the annual models as well as illustrates that the relationships between teleconnections, their interactions, and tornado activity vary across the seasons (Table 2).

As seen at the annual scale, the AO:NAO interaction was chosen as a predictor of tornado activity in DJF. The selection of AO in the DJF model aligns with Childs et al. (2018), who reports a positive relationship between tornado activity and AO in the cold season, but we show here that the interaction with NAO modulates this relationship. Specifically, the odds ratios of the DJF model indicate that the probability of an active season decreases with AO as values of the NAO index increase. In fact, the probability of an active season moves from near 0% for an AO value of − 2 to at least 75% with an AO value of 2 across the entire interquartile range of NAO values.

Coming out of the cold season and into the spring, NAO is still selected as a predictor, but as an interaction with ENSO rather than AO. The interaction plots shown in Fig. 3A illustrate that the greatest probabilities for an active season occur when ENSO and NAO are in opposite phases. Put another way, the probability of an active season is highest during La Niña with positive values of NAO or during El Niño with negative values of NAO.

By summer, the relationship between tornado activity and multiple teleconnections weakens. In the JJA model only PNA is chosen as an independent predictor of high tornado activity. The *beta* coefficient and odds ratios of JJA model suggests that the probability of an active season decreases with higher values of the PNA index. Quantitatively, the probability of an active season moves from near 70% for a PNA value of − 1 to near 30% with a PNA value of 1.

In fall, this simple relationship between a single predictor and tornado activity becomes more complex as the SON model having the highest number of predictors and interactions. In fact, ENSO, AO, NAO, and PNA were all selected for the most parsimonious model with ENSO:AO and AO:PNA interactions included. The interaction term including ENSO and AO was the most significant term in the model, highlighting the influence ENSO has on tornado activity across multiple seasons. The ENSO:AO interaction shown in Fig. 3B), with the greatest probability of an active season occurring when ENSO and AO are in opposite phases, is similar to the joint ENSO and AO effect reported by Tippett et al. (2022) but also suggests that the ENSO:AO interaction may occur in other seasons and is not confined to February, March, and April.

3.3 Monthly models

Moving beyond an annual or seasonal modeling approach, we subset our original data set of 828 unique combinations of year, month, and period by month and estimate a monthly model. As seen in the seasonal models, the teleconnections and teleconnection interactions selected in the stepwise process vary across the months. At the more granular monthly scale, these models also illustrate sub-seasonal variability in some of the teleconnection/tornado relationships, suggesting scale dependence of these relationships (Table 2). The AO:NAO interaction, for example, detected in the DJF model is seen only in January, whereas NAO and AO are independent predictors in December and February, respectively. Likewise, the ENSO:NAO interaction from the MAM model is identified only in the April model and the AO:PNA interaction from SON is identified only in November.

In several fall and winter months, the most parsimonious models illustrate the previously reported importance of La Niña conditions to tornado activity in the SE US. They also indicate that ENSO interacts with other teleconnections, like PNA and NAO, to modulate tornado activity. In September and November, for example, active months are favored when the teleconnections are jointly negative whereas strong positive PNA and NAO reduce the odds that a month will be active—even when La Nina conditions are present (Fig. 4A, 4B). In February, ENSO also interacts with PNA and NAO to drive some level of tornado activity (Fig. 4C). That said, the impact of ENSO is more evident than either of PNA or NAO, as an active month is favored during La Niña conditions across a larger portion of the PNA and NAO spectrums.

Transitioning into spring, ENSO continues to be an important predictor as seen with other studies, but the April and May models again suggest interaction with other teleconnections. In April, an active month is favored during La Niña but only when NAO is positive and AO is slightly positive or negative (Fig. 5A). As in April, active Mays are also more likely when La Niña conditions are present, but only when AO is relatively neutral or positive and when PNA is weakly negative to positive (Fig. 5B). Despite the importance of ENSO, the April and May models suggest that an active month is likely even during El Niño conditions if other teleconnections are suitable (e.g., negative NAO in April and negative AO in May).

As found in other studies (e.g., Moore 2018), the statistical relationship between ENSO and tornado activity seems to flip in summer when active months are most favored during the El Niño state. However, the monthly models performed here suggest that this reversal occurs only in early summer and is contingent on interactions with NAO and AO, with the greatest probability for an active June associated with the coupling of El Niño conditions with negative NAO and AO (Fig. 6). Like the JJA model, PNA is selected as an independent predictor in June and July.

4 Discussion

Understanding the relationship between teleconnections and tornado activity is an important scientific question. It relies on the availability of longitudinal data for climate variables and tornadoes that exist spatially and at scale. Here we develop statistical models for tornado activity at an annual, seasonal, and monthly level using a suite of teleconnections and their interactions as the included parameters. Through

a data-driven approach, we identify which teleconnections and interactions best predict whether a year, season, or month is likely to be active.

Previous literature has identified a seasonal relationship between teleconnections and tornadoes (Elsner et al. 2016; Childs et al. 2018; Moore 2018; Brown and Nowotarski 2020; Nouri et al. 2021; Tippett et al. 2022). Here, we find a similar relationship through model selection that includes the greatest number of teleconnections and interactions and the highest estimated magnitude of effect on tornado activity in late winter through spring and into early summer (Fig. 7). In late summer through early fall, however, model selection returns relatively fewer teleconnections as predictors of tornado activity. In agreement with other seasonal-scale studies (Moore 2019), the monthly models show a weakening ENSO signal in summer, while also indicating that NAO and AO are less important to tornado activity in late summer and early fall. This weakening or lack of a teleconnection signal in late summer and early fall aligns with work suggesting that summer convective activity can be driven by short-term and sub-synoptic scale processes (Gaal and Kinter III 2021) and is suggestive of difficulties with sub-seasonal-to-seasonal tornado outlooks (Gensini et al. 2020) extended into summer. Like the other teleconnections, PNA seems less important to tornado activity in summer and fall but is retained in more monthly models between July and December than any other teleconnections, indicating that PNA might outperform others when predicting the odds of an active month during summer or early fall.

Visual inspection of environmental conditions during phase interactions of teleconnections that are associated with high predicted probabilities of active tornado periods can provide additional insight into possible physical mechanisms. Perhaps best seen at the monthly level, climate composites can be used to illustrate potential physical mechanisms contributing to tornado-active environments. For example, the ENSO:PNA interaction in February is a significant predictor of an active tornado month (Table 2). The highest probability of an active February occurs when both ENSO and PNA are negative (Fig. 4). In fact, the distribution of active months is clearly seen with negative ENSO-negative PNA values and the median number of tornadoes is highest in February with a negative ENSO-negative PNA relationship (Fig. 8A, B). Physical explanations for an above active month during a negative ENSO-negative PNA interaction include anomalously high 850-mb geopotential heights over portions of the SE US and southwestern Atlantic, which sets the stage for anomalously high 2-m air temperature and specific humidity across the region (Fig. 8C, D, E).

The ENSO:NAO interaction in April is a significant predictor of an active tornado month. Unlike February, however, the highest probability occurs when both teleconnections are in opposite phases (Fig. 5). This suggests that there are four possible phase combinations to drive an active or inactive April: (1) negative ENSO-positive NAO, (2) negative ENSO-negative NAO, (3) positive ENSO-positive NAO, and (4) positive ENSO-negative NAO. The empirical probabilities of an active April with negative ENSO-positive NAO and positive ENSO/negative NAO conditions are 60% or greater whereas the probability of an active month when both teleconnections are in the same phase is at or below 50% (Fig. 9A, B). In addition, the median number of tornadoes with opposite phase ENSO-NAO relationships are higher than either of the same phase ENSO-NAO relationships (Fig. 9B). The climate conditions associated with the active negative

ENSO-positive NAO interaction are similar to those seen with the negative ENSO/negative PNA interaction in February, with anomalously high 850-mb geopotential heights, 2-m air temperature, and 2-m specific humidity across the SE US (Fig. 9C, D, E). Conversely, the climate conditions associated with the active positive ENSO-negative NAO interaction are opposite with anomalously low heights, temperature, and specific humidity across the continental US (Fig. 9F, G, H).

The ENSO:AO interaction in June is a significant predictor of an active tornado month. Similar to April, the highest probability occurs when both teleconnections are in opposite phases (Fig. 6). The empirical probabilities of an active June are notably higher when ENSO and AO are in opposite phases than when ENSO and AO are in the same-signed phase (Fig. 10A, B). Additionally, the median number of tornadoes with opposite phase ENSO-AO relationships are higher than either of the same phase ENSO-NAO relationships (Fig. 10B). When ENSO is positive and AO is negative, climate conditions across the SEUS are characterized by anomalously low 850-mb geopotential heights, near-normal 2-m air temperature, and anomalously high 2-m specific humidity (Fig. 10C, D, E).

Moving forward, work will be needed to investigate the physical relationships between teleconnections and tornado activity as a means of explaining potential causal mechanisms between environmental conditions and these data driven models. In this sense, research could move beyond a purely statistical approach toward a physical approach by determining if and how synoptic or mesoscale patterns and tornado-favorable ingredients vary across bivariate states of teleconnection interactions. As seen in the preliminary analysis of the ENSO:PNA, ENSO:NAO, and ENSO:AO interactions for February, April, and June, respectively, physical mechanisms across the entire range of teleconnection indices can contribute to greater-than-normal tornado activity. For instance, anomalously high near-surface temperature and humidity steered by an active subtropical high near the SE US is likely leading to more active environments. That said, not all interactions are characterized by these environments. Additional study is necessary to tease out the complex ways in which climate patterns work both independently and interactively to modulate tornado activity (Brown and Nowotarski 2020; Tippett et al. 2022).

5 Conclusions

The United States experiences more tornadoes, on average, than any other country on Earth. Recent research has shown that tornado climatology is changing over time, with decreased activity in the Great Plains and increased activity in the SE US. Some studies have looked to link large-scale climate patterns and tornadoes through a monthly or seasonal outlook, while others have explored the relationship between multiple teleconnections and tornadoes across the entirety of the United States. Here, we deviate from those works by developing statistical models aimed at predicting above or below normal tornado activity in the SE US through teleconnections and their interactions at an annual, seasonal, and monthly level. In particular, we develop logistic regression models that incorporate a suite of teleconnections and their interactions fit to data that accounts for non-stationarity across multiple time periods.

The data-driven modeling approach outlined identifies the most parsimonious models as determined by AIC. These selected models yield results aligned with other research, but also highlight potential interactions and sub-seasonal variability not found in the literature. For example, while ENSO was selected in numerous winter and spring monthly models—consistent with prior work—it was often included as an interaction with other teleconnections rather than a singular predictor. This means that ENSO in conjunction with other teleconnections likely affects the probability of an active period greater than ENSO alone. Likewise, AO was selected as a predictor of greater-than-normal tornado activity in April, May, and June not as an independent predictor, but as an interaction with ENSO in all three months and with PNA in April.

The inclusion of interaction terms in the selected models provides an opportunity to move beyond our traditionally understood individual predictors. Rather than focusing on a single teleconnection across the entire range of its values, these models suggest that a combination of teleconnections—in similar phases or opposite phases—provide better predictions of tornado activity. Future work should look to use this statistical evidence as the basis for research centered around physical explanations or hypotheses for how teleconnection interactions provide environments capable of—or not capable of—producing above-normal tornado activity.

Additionally, it is likely that model selection is highly dependent on scale in both time and space. More research should be devoted to using this same approach to tornadoes in other regions of the United States and over shorter time scales, which would open the possibility to incorporate additional teleconnections (e.g., Madden-Julian Oscillation). Such efforts might help identify the optimum scales over which these relationships exist and shed insight into why some periods have high/low tornado activity even during unfavorable/favorable background states.

Declarations

Author Contribution

T.W.M, T.A.D, and T.F. conceived of the study and study design. T.W.M and T.A.D performed statistical analysis and generated figures and tables. T.W.M, T.A.D, and T.F reviewed and wrote portions of the manuscript.

Acknowledgements

Support for the 20th Century Reanalysis Project version 3 dataset is provided by the U.S. Department of Energy, Office of Science Biological and Environmental Research (BER), by the National Oceanic and Atmospheric Administration Climate Program Office, and by the NOAA Earth System Research Laboratory Physical Sciences Laboratory.

References

1. Agee E, Larson J, Childs S, Marmo A (2016) Spatial redistribution of U.S. tornado activity between 1954 and 2013. J Appl Meteorol Climatology 55:1681–1697. 10.1175/JAMC-D-15-0342.1
2. Alexander MA, Bladé I, Newman M, Lanzante JR, Lau NC, Scott JD (2002) The atmospheric bridge: The influence of ENSO teleconnections on air–sea interaction over the global oceans. J Clim 15:2205–2231
3. Allen JT, Tippett MK, Sobel AH (2015) Influence of El Niño-Southern Oscillation on tornado and hail frequency in the United States. Nat Geosci 8:278–283. 10.1038/ngeo2385
4. Ashley W (2007) Spatial and temporal analysis of tornado fatalities in the United States: 1880–2005. Weather Forecast 22:1214–1228. 10.1175/2007WAF2007004.1
5. Ashley WS, Strader SM (2016) Recipe for disaster: How the dynamic ingredients of risk and exposure are changing the tornado disaster landscape. Bull Am Meteorol Soc 97:767–786
6. Brooks HE, Doswell CA III (2002) Deaths in the 3 May 1999 Oklahoma City tornado from a historical perspective. Weather Forecast 17:354–361
7. Brown MC, Nowotarski CJ (2020) Southeastern U.S. tornado outbreak likelihood using daily climate indices. J Clim 33:3229–3252
8. Changnon SA (2009) Tornado losses in the United States. Nat Hazards Rev 10:145–150
9. Chaurasia A, Harel O (2012) Using AIC in multiple linear regression framework with multiply imputed data. Health Serv Outcomes Res Method 12:219–233
10. Childs SJ, Schumacher RS, Allen JT (2018) Cold-season tornadoes: Climatological and meteorological insights. Weather Forecast 33:671–691
11. Coleman TA, Dixon PG (2014) An objective analysis of tornado risk in the United States. Weather Forecast 29:366–376
12. Cook AR, Leslie LM, Parsons DB, Schaefer JT (2017) The impact of El Niño–Southern Oscillation (ENSO) on winter and early spring US tornado outbreaks. J Appl Meteorol Climatology 56:2455–2478
13. Cutter SL, Boruff BJ, Shirley WL (2003) Social vulnerability to environmental hazards. Soc Sci Q 84:242–261
14. Dixon PG, Mercer AE, Choi J, Allen JS (2011) Tornado risk analysis: Is Dixie alley an extension of tornado alley? Bull Am Meteorol Soc 92:433–441
15. Deser C (2000) On the teleconnectivity of the Arctic Oscillation. Geophys Res Lett 27:779–782
16. DeBoer TA (2019) Relationships between teleconnections and tornado activity in the southeastern United States. Thesis. Towson University
17. Elsner JB, Jagger TH, Fricker T (2016) Statistical models for tornado climatology: Long and short-term views. PLoS ONE 11:e0166895

18. Elsner JB, Fricker T, Berry WD (2018) A model for US tornado a = casualties involving interaction between damage path estimates of population density and energy dissipation. J Appl Meteorol Climatology 57:2035–2046
19. Fricker T, Elsner J (2019) Unusually devastating tornadoes in the United States: 1995–2016. Annals Am Association Geographers 110:724–738. 10.1080/24694452.2019.1638753
20. Fricker T, Friesenhahn C, Weather (2022) Clim Soc 14: 81–93. doi: 10.1175/WCAS-D-21-0028.1
21. Gaal R, Kinter JL III (2021) Soil moisture influence on the incidence of summer mesoscale convective systems in the U.S. Great Plains. Mon Weather Rev 149:3981–3994
22. Gensini VA, Brooks HE (2018) Spatial trends in United States tornado frequency. NPJ Clim Atmospheric Sci 1:38. 10.1038/s41612-018-0048-2
23. Gilford DM, Smith SR, Griffin ML, Arguez A (2013) Southeastern US Daily Temperature Ranges Associated with the El Niño–Southern Oscillation. J Appl Meteorol Climatology 52:2434–2449
24. Gijben M, Dyson LL, Loots MT (2017) A statistical scheme to forecast the daily lightning threat over southern Africa using the Unified Model. Atmos Res 194:78–88
25. Glickman TS, Walter Z (2000) Glossary of Meteorology, 855 edn. American Meteorological Society
26. Gorsevski PV, Gessler PE, Foltz RB, Elliot WJ (2006) Spatial prediction of landslide hazard using logistic regression and ROC analysis. Trans GIS 10:395–415
27. Guo L, Wang K, Bluestein HB (2016) Variability of tornado occurrence over the continental United States since 1950. J Geophys Research: Atmos 121:6943–6953
28. Leathers DJ, Yarnal B, Palecki MA (1991) The Pacific/North American teleconnection pattern and United States climate. Part I: Regional temperature and precipitation associations. J Clim 4:517–528
29. Lepore C, Tippett MK, Allen JT (2017) ENSO-based probabilistic forecasts of March–May U.S. tornado and hail activity. Geophys Res Lett 44:9093–9101. 10.1002/2017GL074781
30. Marzban C, Schaefer JT (2001) The correlation between US tornadoes and Pacific sea surface temperatures. Mon Weather Rev 129:884–895
31. Moore TW (2018) Annual and seasonal tornado trends in the contiguous United States and its regions. Int J Climatol 38:1582–1594. 10.1002/joc.5285
32. Moore TW (2019) Seasonal frequency and spatial distribution of tornadoes in the United States and their relationships to the El Niño/Southern Oscillation. Annals Am Association Geographers 109:1033–1051. 10.1080/24694452.2018.1511412
33. Moore TW, St. Clair JM, DeBoer TA (2018) An analysis of anomalous winter and spring tornado frequency by phase of the El Nino/Southern Oscillation, the Global Wind Oscillation, and the Madden-Julian Oscillation. Advances in Meteorology. 10.1155/2018/3612567
34. Moore TW, DeBoer TA (2019) A review and analysis of possible changes to the climatology of tornadoes in the United States. Progress Phys Geography: Earth Environ 43:365–390. 10.1177/0309133319829398

35. Munoz E, Enfield D (2011) The boreal spring variability of the Intra-Americas low-level jet and its relation with precipitation and tornadoes in the eastern United States. Clim Dyn 36:247–259
36. NOAA (2018a) Climate Weather Linkage: Teleconnections. https://www.cpc.ncep.noaa.gov/products/precip/CWlink/daily_ao_index/teleconnections.shtml. Accessed 4 February 2024
37. NOAA (2018b) Niño 3.4 SST Index. Earth System Research Laboratory. https://www.esrl.noaa.gov/psd/gcos_wgsp/Timeseries/Nino34/. Accessed 4 February 2024
38. Nouri N, Devineni N, Were V, Khanbilvardi R (2021) Explaining the trends and variability in the United States tornado record using climate teleconnections and shifts in observational practices. Nat Sci Rep 11:1741. 10.1038/s41598-81143-5
39. Smith TM, Reynolds RW, Livezey RE, Stokes DC (1996) Reconstruction of historical sea surface temperatures using empirical orthogonal functions. J Clim 9:1403–1420
40. SPC (2018) Storm Prediction Center WCM Page. https://www.spc.noaa.gov/wcm/. Accessed 4 February 2024
41. Strader SM, Ashley WS, Pingel TJ, Krmenec AJ (2017) Observed and projected changes in United States tornado exposure. Weather Clim Soc 9:109–123
42. Ting M, Hoerling MP, Xu T, Kumar A (1996) Northern Hemisphere teleconnection patterns during extreme phases of the zonal-mean circulation. J Clim 9:2614–2633
43. Tippett MK, Lepore C, L'Heureux ML (2022) Predictability of a tornado environmental index from El Nino-Southern Oscillation (ENSO) and the Arctic Oscillation. Weather Clim Dynamics 3:1063–1107. 10.5194/wcd-3-1063-2022
44. Verbout SM, Brooks HE, Leslie LM, Schultz DM (2006) Evolution of the US tornado database: 1954–2003. Weather Forecast 21:86–93

Figures

Figure 1

Study area. The state boundaries of those defined as the Southeast are shaded in grey.

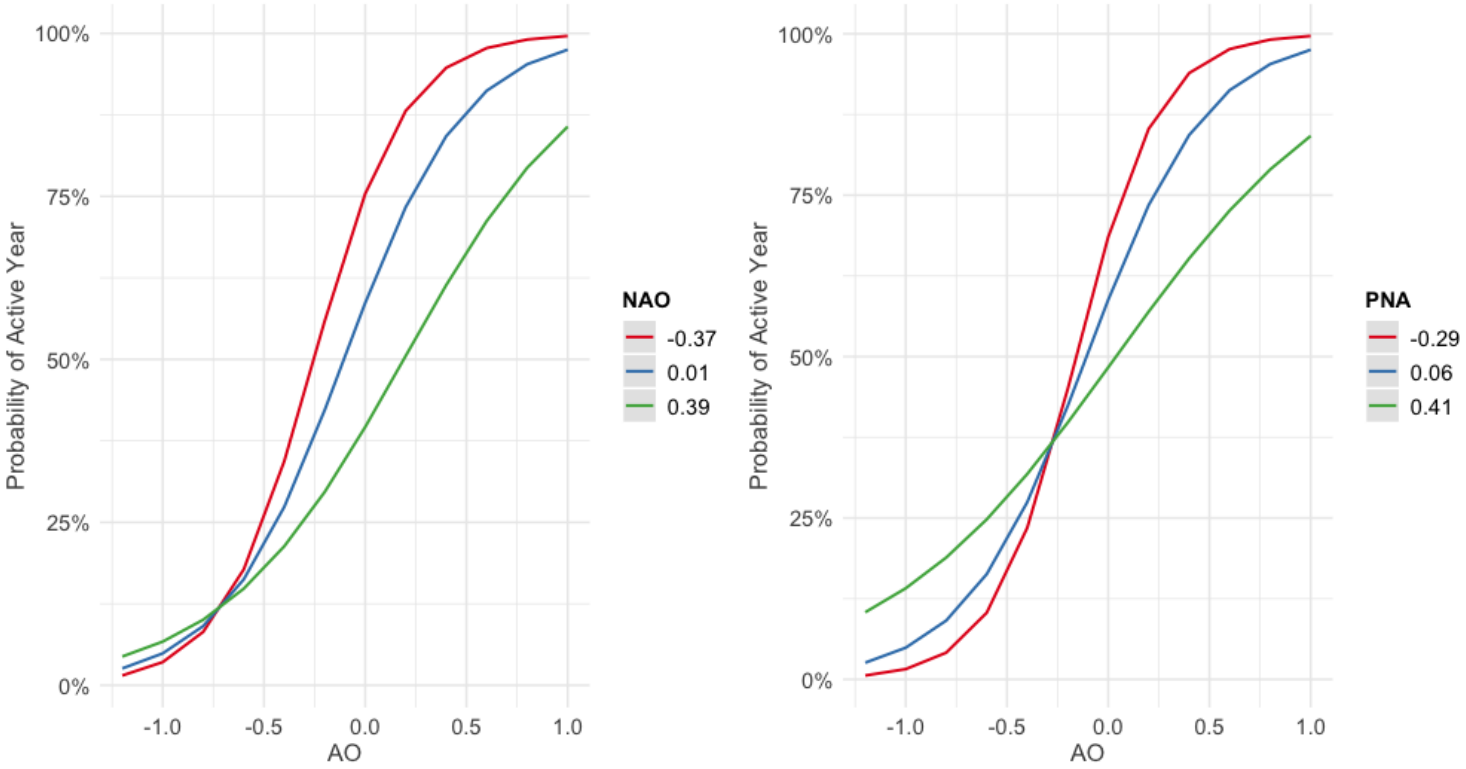

Figure 2

Predicted probabilities (marginal effects) of an active year based on interactions between AO and NAO, and AO and PNA. Values of the NAO and PNA indices represent the 25th, 50th, and 75th percentiles.

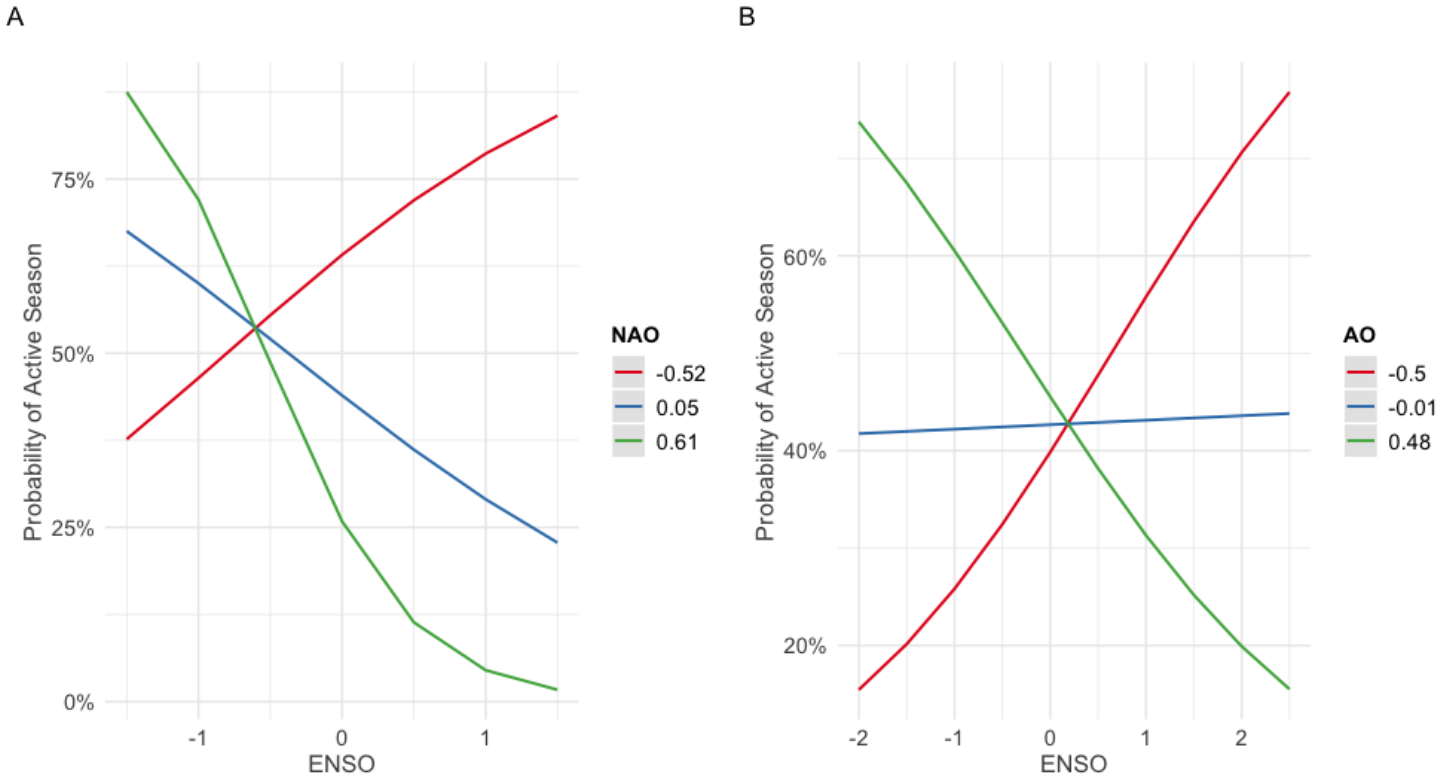

Figure 3

Predicted probabilities (marginal effects) of an active season for (A) MAM based on ENSO and NAO, and (B) SON based on ENSO and AO. Values of the NAO and AO indices represent the 25th, 50th, and 75th percentiles.

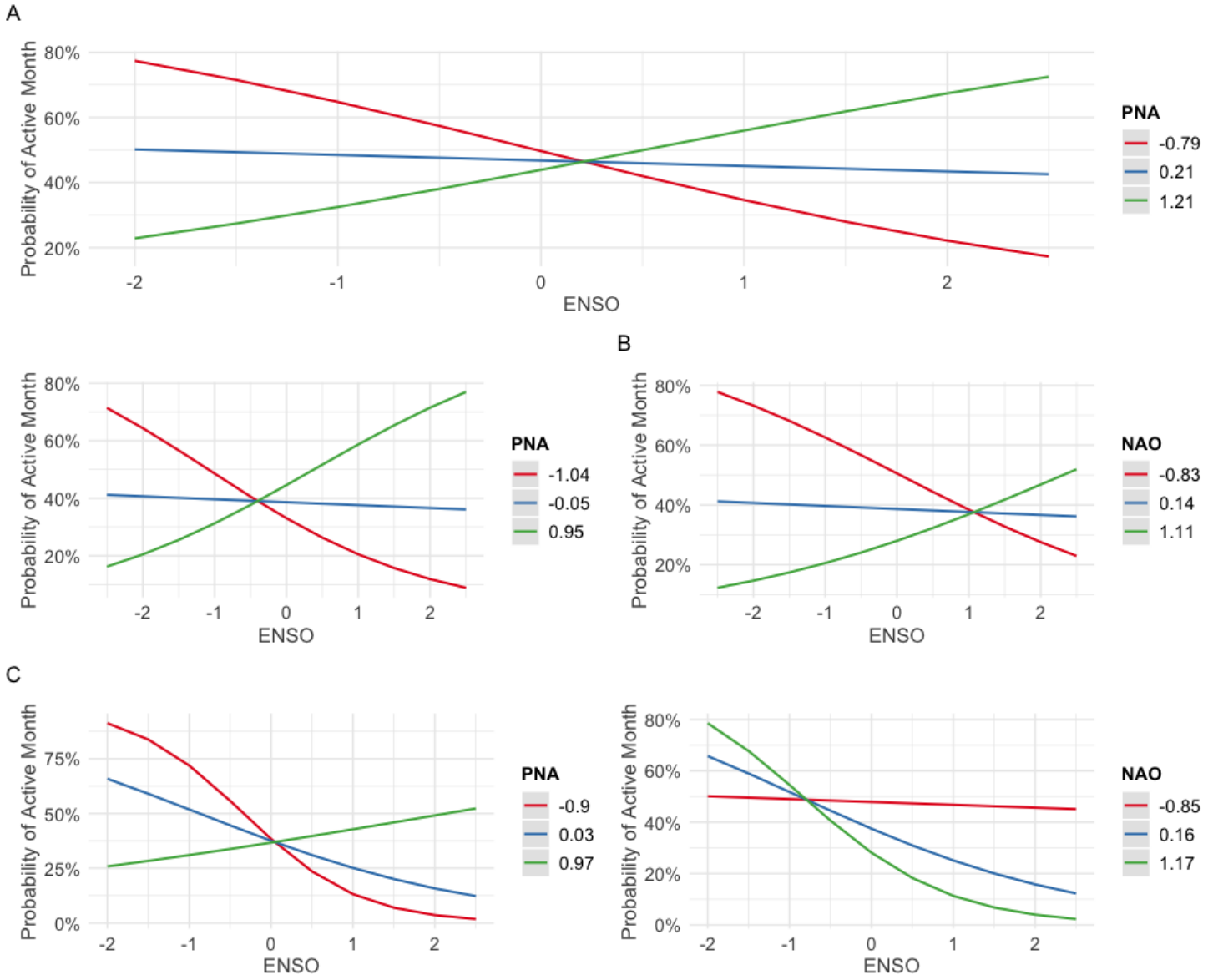

Figure 4

Predicted probabilities (marginal effects) of an active (A) September, (B) November, and (C) February based on interactions between ENSO and PNA and NAO. Values of the PNA and NAO indices represent the 25th, 50th, and 75th percentiles.

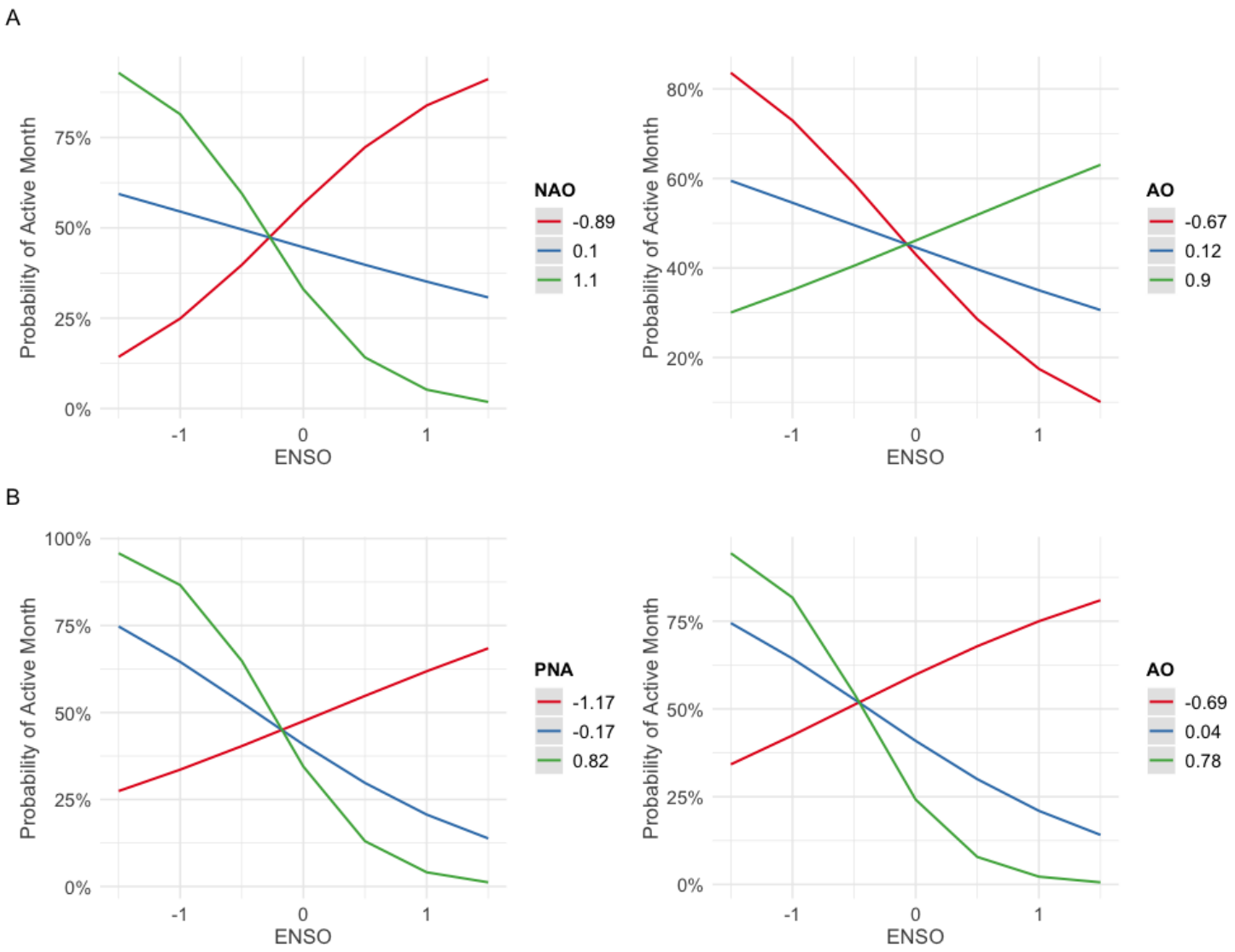

Figure 5

Predicted probabilities (marginal effects) of an active (A) April and (B) May based on interactions between ENSO and NAO, AO, and PNA. Values of the NAO, AO, and PNA indices represent the 25th, 50th, and 75th percentiles.

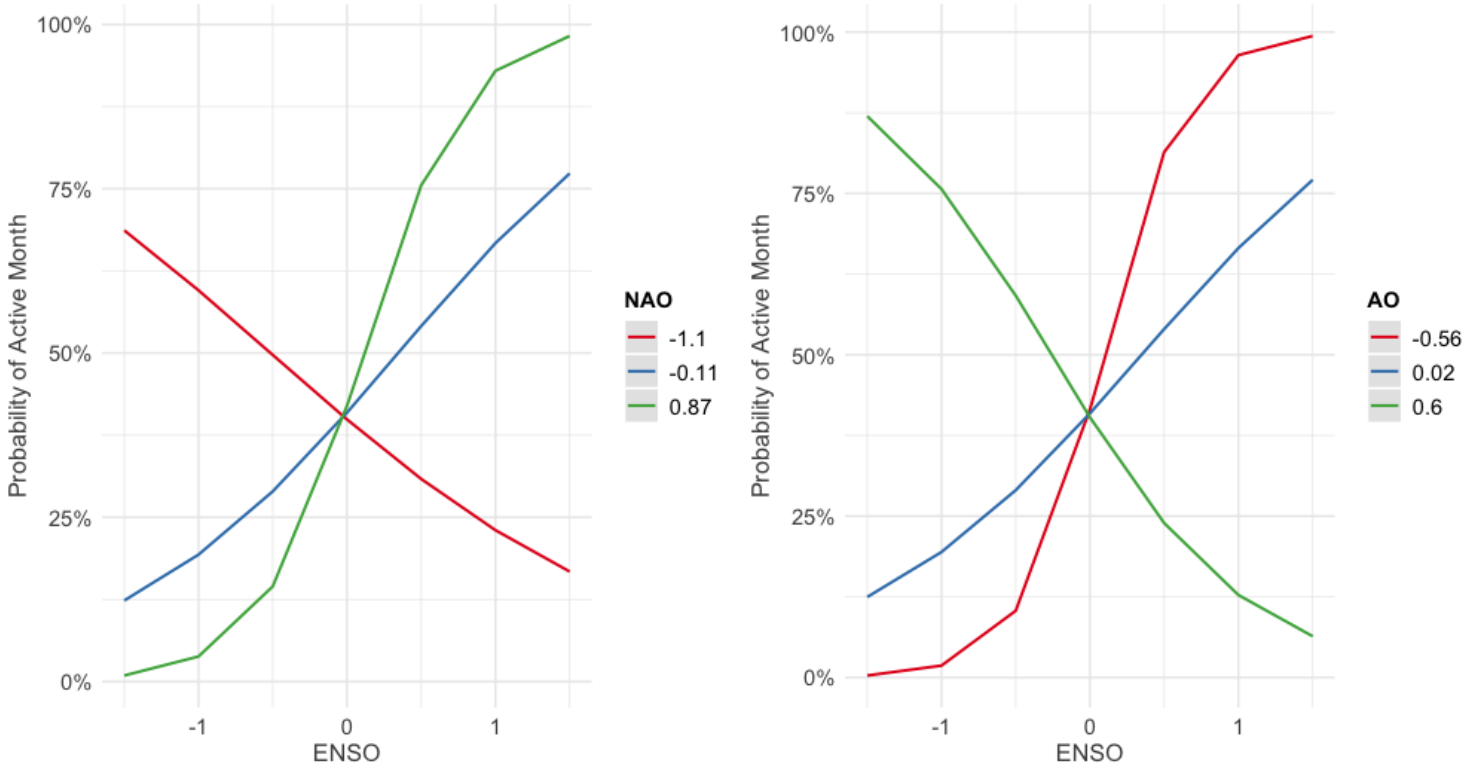

Figure 6

Predicted probabilities (marginal effects) of an active June based on interactions between ENSO and NAO and AO. Values of the NAO and AO indices represent the 25th, 50th, and 75th percentiles.

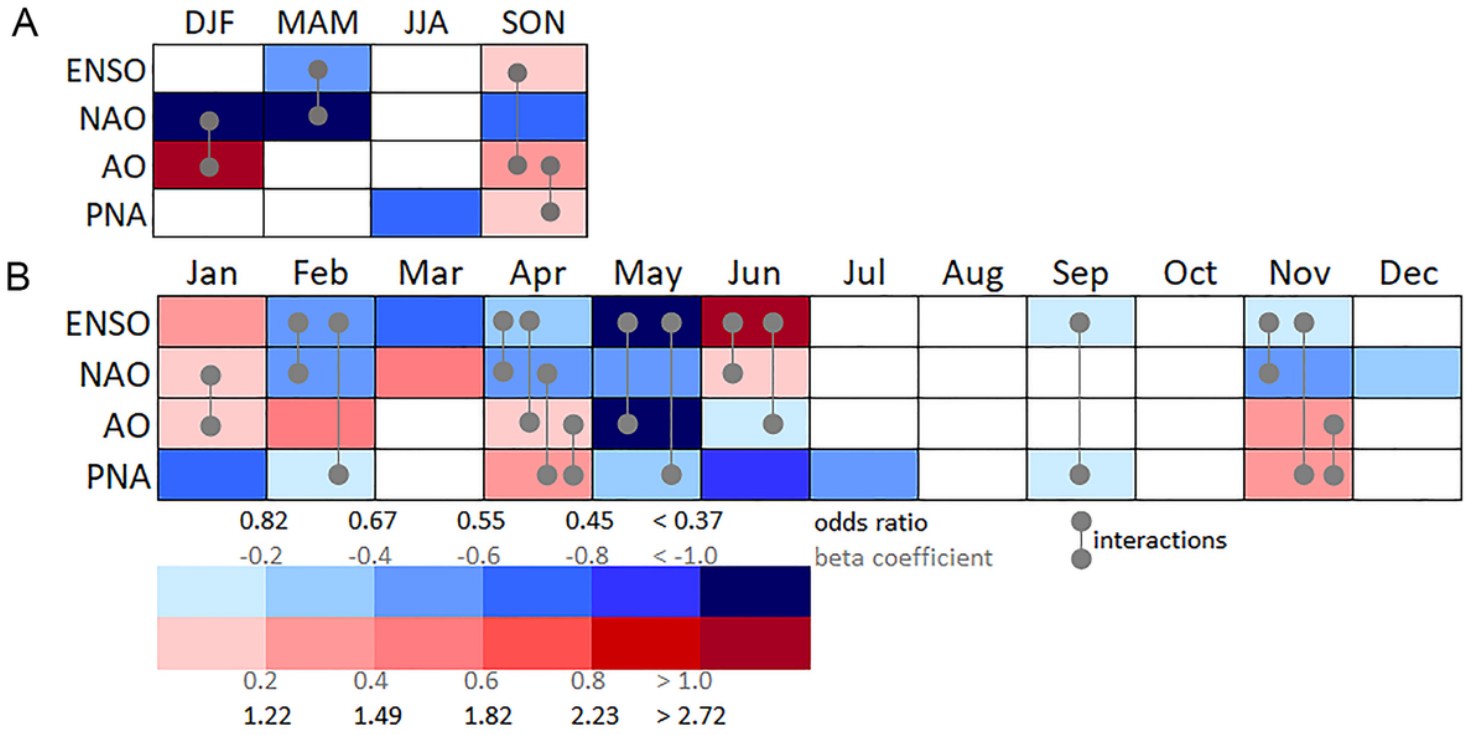

Figure 7

Visualization of *beta*coefficients, odds ratios, and teleconnection interactions for (A) seasonal and (B) monthly logistic regression models, with teleconnections and their interactions as predictors and tornado activity as the predictand. Blues indicate negative odds ratios while reds indicate positive odds ratios. The interactions are highlighted by grey line segments.

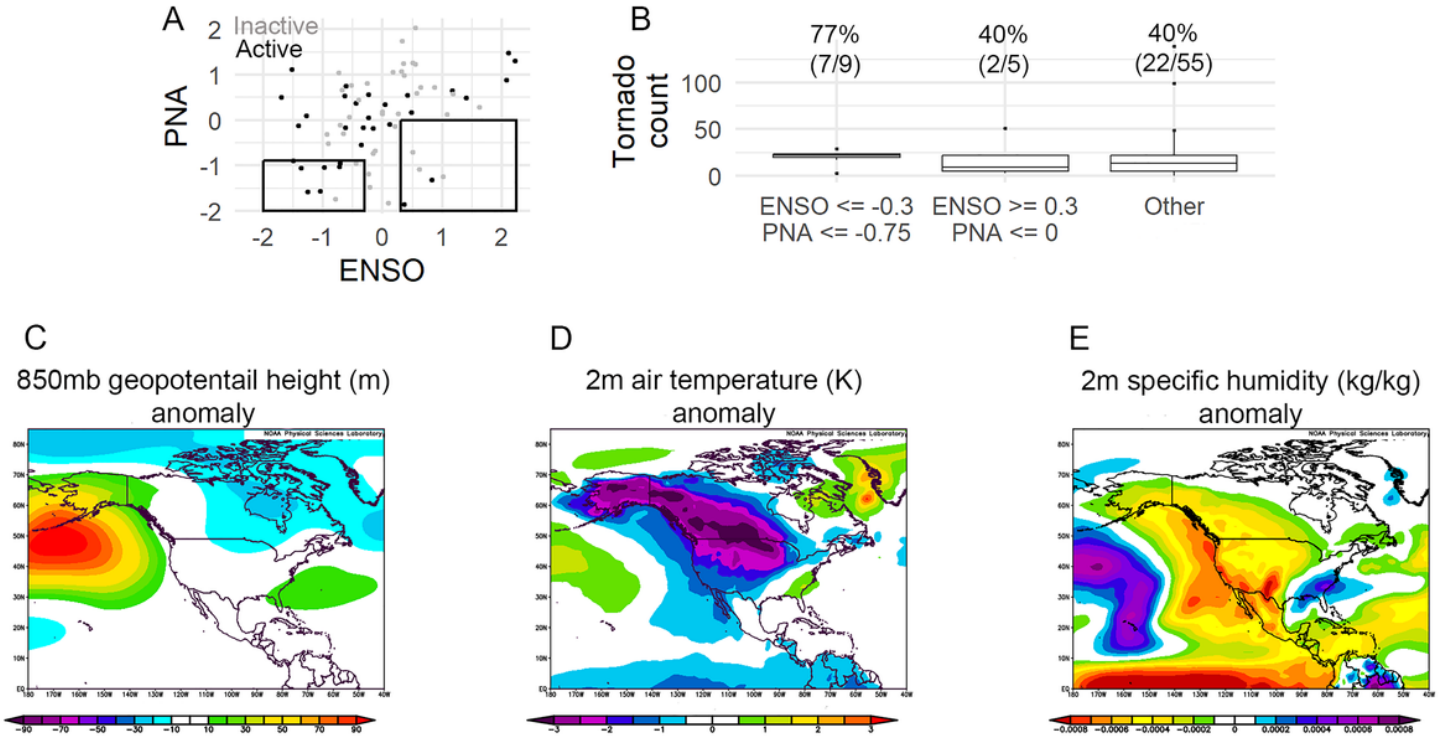

Figure 8

(A) February tornado activity as a function of ENSO and PNA, with active months shown in black and inactive months shown in grey. Polygons are estimated from the probabilities shown in Figure 4C. (B) Bivariate distributions of February tornado counts. Categories correspond to polygons in panel A. Probabilities of an active month per category are provided as %s. (C–E) Climate conditions corresponding to the tornado-active negative ENSO/negative PNA (ENSO ≤ -0.3, PNA ≤ -0.75) interaction. Years included in these composites include 1955, 1956, 1974, 1976, 1989, 2009, 2011, 2014, and 2018.

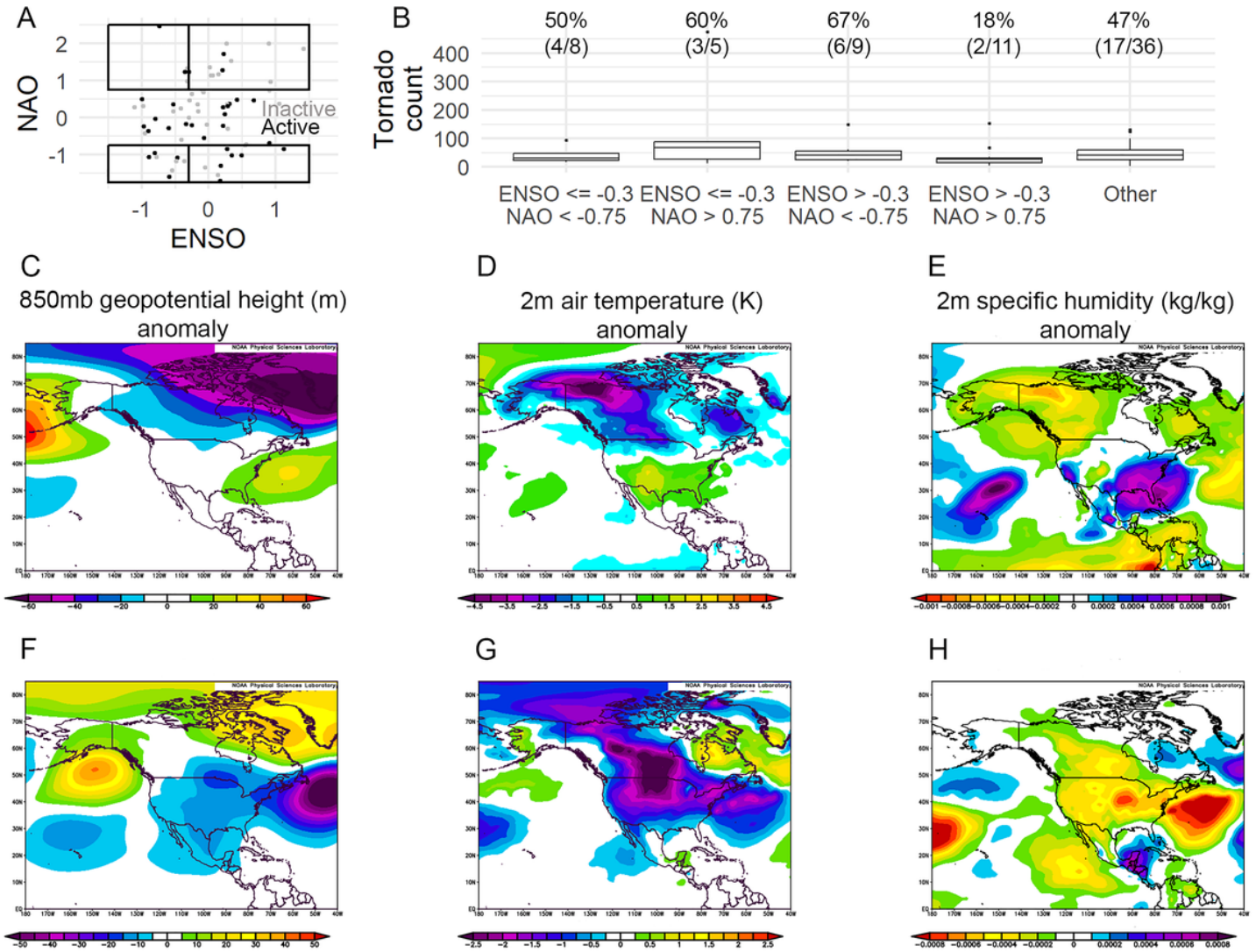

Figure 9

(A) April tornado activity as a function of ENSO and NAO, with active months shown in black and inactive months shown in grey. Polygons are estimated from the probabilities shown in Figure 5A. (B) Bivariate distributions of April tornado counts. Categories correspond to polygons in panel A. Probabilities of an active month per category are provided as percentages. (C–E) Climate conditions corresponding to the tornado-active negative ENSO/positive NAO (ENSO ≤ -0.3, NAO ≥ 0.75) interaction. Years included in these composites include 1954, 1962, 2006, 2011, and 2018. (F–H) Climate conditions corresponding to the tornado-active positive ENSO/negative NAO (ENSO > -0.3, NAO < -0.75) interaction. Years included in these composites include 1961, 1963, 1970, 1979, 1983, 1995, 1997, and 2020.

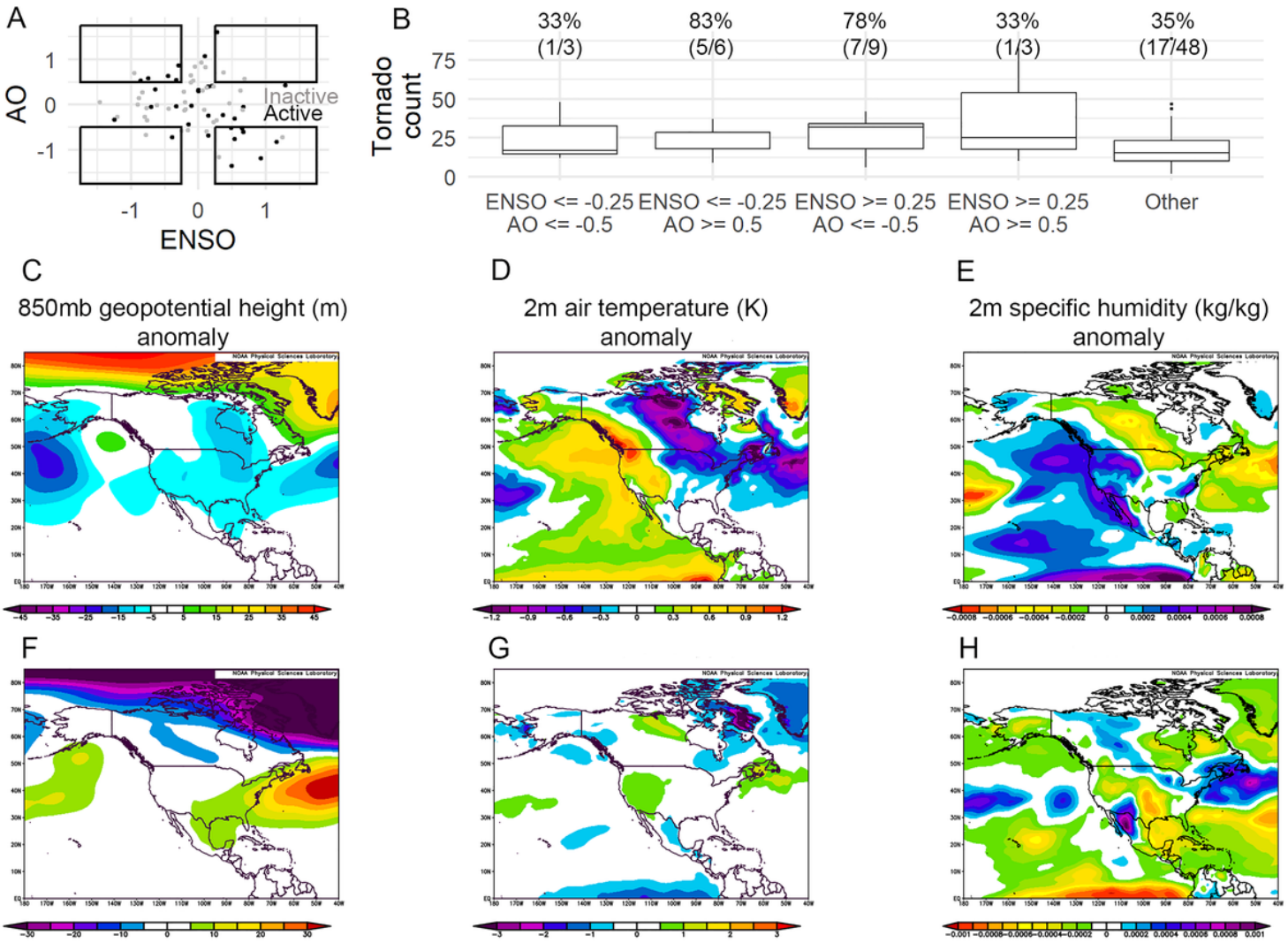

Figure 10

(A) June tornado activity as a function of ENSO and AO, with active months shown in black and inactive months shown in grey. Polygons are estimated from the probabilities shown in Figure 6. (B) Bivariate distributions of June tornado counts. Categories correspond to polygons in panel A. Probabilities of an active month per category are provided as %s. (C–E) Climate conditions corresponding to the tornado-active positive ENSO/negative AO (ENSO ≥ 0.25, AO ≤ -0.5) interaction. Years included in these composites include 1957, 1958, 1982, 1987, 1993, 1997, 2009, 2014, and 2019. (F–H) Climate conditions corresponding to the tornado-active negative ENSO/positive AO (ENSO ≤ -0.25, AO ≥ 0.5) interaction. Years included in these composites include 1970, 1973, 1978, 1999, 2000, and 2013.